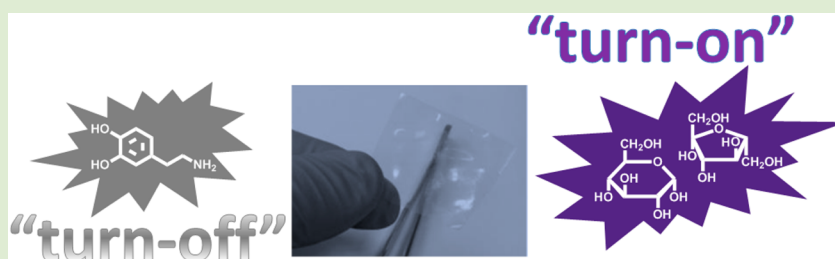


# Acrylic Polymers with Pendant Phenylboronic Acid Moieties as “Turn-Off” and “Turn-On” Fluorescence Solid Sensors for Detection of Dopamine, Glucose, and Fructose in Water

Jesús L. Pablos,<sup>†</sup> Saúl Vallejos, Saturnino Ibeas, Asunción Muñoz, Felipe Serna, Félix C. García, and José M. García\*

Departamento de Química, Facultad de Ciencias, Universidad de Burgos, Plaza de Misael Bañuelos s/n, 09001 Burgos, Spain

## S Supporting Information



**ABSTRACT:** We report herein a fluorescence polymer membrane as a film-shaped solid sensory kit for the detection and quantification in water of saccharides, namely, fructose and glucose, and dopamine. The sensory motifs are phenylboronic acids, which are chemically incorporated in the polymer network in the radically initiated bulk polymerization process. The sensory membrane is fluorescent. The interaction of the sensory motifs with dopamine “turn-off” the fluorescence due to a dynamic quenching, while stable complexes are formed with saccharides giving rise to a fluorescence “turn-on”. The variation of the fluorescence intensity and the wavelength of the maxima permitted the titration of the species with a detection limit of  $3\text{--}4 \times 10^{-4}$  M. The hydrophilic membrane allowed for the detection in water in spite of the lack of solubility in this medium of the sensory phenylboronic acid derivative monomer.

There is considerable interest in the synthesis, design, and application of sensory polymeric materials for the detection of different types of biomolecules with important roles in life processes. Among such biologically relevant molecules are the dopamine and saccharide (carbohydrate) family. Dopamine, the shortened form of 3,4-dihydroxyphenethylamine, is a neurotransmitter that plays important roles in the human body and brain, e.g., as a monoamine neurotransmitter in movement control, emotional responses, and the faculty to sense pleasure or pain, and is also a biomarker and a treatment in certain diseases.<sup>1–4</sup> On the other hand, saccharide molecules have vital roles in many biological processes, and their monitoring, e.g., the D-glucose levels in the blood of diabetic patients, is of the utmost importance.<sup>5,6</sup> The search for reliable and sensitive, inexpensive, and rapid nonenzymatic sensors for the detection of glucose in blood serum or saliva is one of the most wanted goals due to the insufficient stability of the enzyme glucose oxidase.<sup>7,8</sup> Furanose saccharides, such as fructose, are important components in a large number of compounds with biological activity such as DNA, RNA, and ribonucleotide cofactors (NAD, NADP) and are fundamental to the cell wall integrity and pathogenicity of many mycobacteria.<sup>9–12</sup>

In recent years, boronic acid derivatives have proven their capability as chemosensors of saccharides, whose 1,2- and 1,3-diol motifs form five- and six-membered cyclic esters in basic

aqueous media.<sup>13–15</sup> Similarly, catechol (1,2-dihydroxybenzene) derivatives, such as dopamine, were reported to give analogous cyclic derivatives upon interaction with boronic acids.<sup>16–20</sup> Following this well-proven strategy as a guarantee of success, and with the objective of preparing solid sensory materials for 1,2- and 1,3-diols, we synthesized a new fluorescent acrylic monomer with pendant phenylboronic acid motifs and prepared a dense membrane by thermally initiated radical polymerization to sense in water dopamine at physiological pH (pH 7) and glucose and fructose in basic medium (pH 10). The solid sensory material showed enhanced fluorescence, i.e., “turn-on” behavior, for the saccharides and quenching, i.e., “turn-off” behavior, for dopamine.

The acrylic monomer with a phenylboronic acid motif (**3**) was prepared following high-yield and straightforward procedures. The synthetic steps are schematically depicted in [Scheme 1](#), and the procedures are described in the [Supporting Information](#) (SI), Section S1. The chemical interaction of **3** with glucose and fructose was evaluated by <sup>1</sup>H NMR using a basic medium DMSO-*d*<sub>6</sub>/KOD (40 wt % in D<sub>2</sub>O) as solvent (380/20 μL in each experiment) and a concentration of **3** of

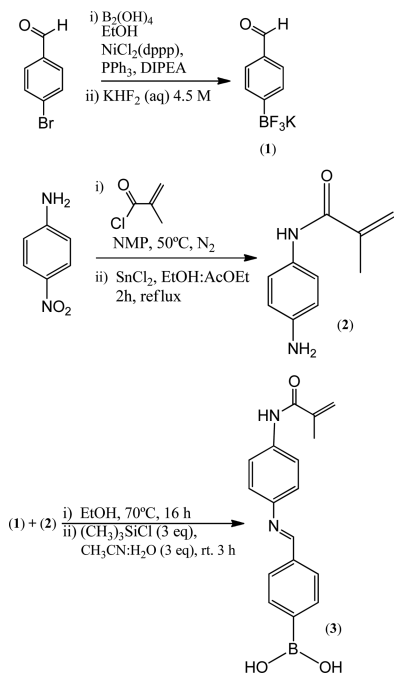
**Received:** July 8, 2015

**Accepted:** August 24, 2015

**Published:** August 25, 2015



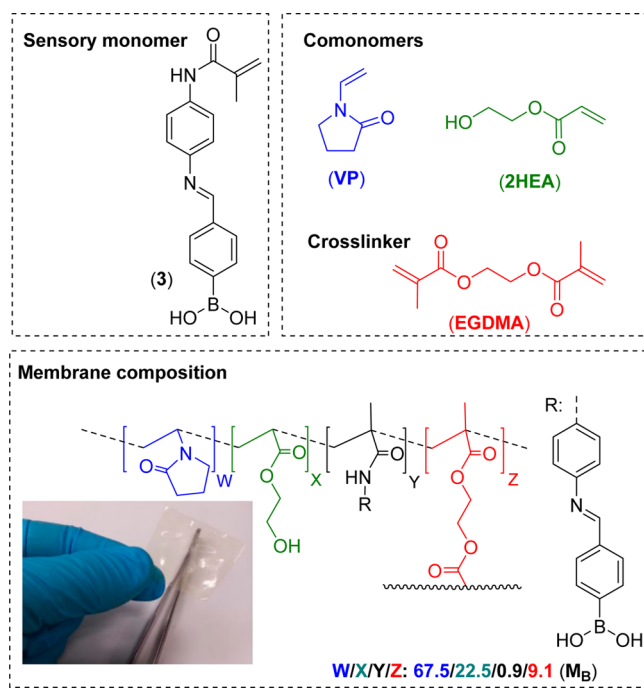
Scheme 1. Synthesis of the Sensory Monomer



0.05 M. In this medium, aromatic signals of **3** split into four doublets by the formation of the  $\text{Ar-B(OH)}_3^-$  species.<sup>21,22</sup> Upon adding increasing quantities of saccharides, changes were observed all along the spectrum until a saccharide to **3** ratio of 1:2 was achieved (SI, Figure S8), in agreement with previously reported complex stoichiometry.<sup>23</sup> On the other hand, the interaction of **3** with dopamine in  $\text{DMSO-}d_6$  was not observed by  $^1\text{H NMR}$  (SI, Figure S9). This fact is in disagreement with the previously reported dopamine–boronic acid sensing mechanism, i.e., static fluorescence quenching,<sup>16–20</sup> but in good agreement with the dynamic quenching proposed below. Neutral conditions were used with dopamine because of its susceptibility to oxidation in basic media.

A 201  $\mu\text{m}$  thick sensory film or membrane ( $M_B$ ) was conventionally prepared by thermally initiated bulk radical copolymerization. Four comonomers were used, and the molar ratio of the sensory monomer (**3**) to the other comonomers, which were commercial, was about 0.9%. The structure of the comonomers, the chemical composition, and a picture of the membrane are depicted in Scheme 2. The used polymerization procedure (thermally initiated radical bulk polymerization with a concomitant addition of monomers) gives usually rise to a random copolymer structure.<sup>24</sup> The membrane composition was designed to be hydrophilic, i.e., to exhibit a gel behavior. This is a requisite because the target molecules (saccharides and dopamine) are in water media (solvated with water) and enter into the membrane by diffusion only if it is water swelled. Inside the membrane, the target species interact with the hydrophobic organic core of **3**, giving rise to the sensing phenomena with the concomitant optical transduction. It is important to consider that **3** is water insoluble and cannot be exploited itself in this medium. The membrane hydrophilic/lipophilic character was related to the solvent-swelling percentage (SSP), that is, to the weight percent of solvent uptake by the films upon soaking them until equilibrium in pure water at rt.  $M_B$  has a SSP of 58% in pure water. It has been proven that a SSP higher than 40% and lower than 100% is

Scheme 2. Chemical Structure of the Sensory Dense Membrane



good for both the rapid diffusion of chemicals into the membrane and for maintaining tractability, in terms of the mechanical properties, of the solvent-swelled acrylic membranes. As a material, the thermal resistance is a key parameter for final applications. It was evaluated thermogravimetrically by TGA. The temperatures that resulted in 5% ( $T_5$ ) and 10% ( $T_{10}$ ) weight loss under a nitrogen atmosphere were 260 and 315  $^\circ\text{C}$ , respectively, indicating that the materials present reasonably good thermal stability. However, the boronic acid moieties exerted great influence in catalyzing the thermal decomposition above 200  $^\circ\text{C}$  as can be seen comparing the decomposition data of a blank membrane (same structure but lacking **3**), which have  $T_5$  and  $T_{10}$  of 369 and 406 K, respectively (SI, Figure S6 and Table S1). The 18% weight loss of  $M_B$  at 370  $^\circ\text{C}$  does not correspond to the small content of pendant phenylboronic acid motifs and could be tentatively ascribed to the loss of fragments derived from the catalytic breakage of ester residues. The FT-IR of  $M_B$  shows the intense bands at 1722 and 1651  $\text{cm}^{-1}$  corresponding to the stretching of the ester and amide  $\text{C}=\text{O}$  bond, respectively. A blank membrane (lacking **3**) showed these bands at 1724 and 1653  $\text{cm}^{-1}$ . The lower and higher energy shifts of ester and amide  $\nu_{\text{C}=\text{O}}$  bands of  $M_B$ , respectively, compared with the blank membrane point out the expected random copolymerization (SI, Figure S7).<sup>24</sup>

The sensing performance of  $M_B$  toward dopamine was studied under neutral conditions (pH = 7, buffer = sodium phosphate monobasic) and toward saccharides under basic conditions (pH = 10, buffer = sodium bicarbonate). Prior to the evaluation of the sensing performance of  $M_B$ , the influence of buffers and UV light on its fluorescence behavior was studied (SI, Section S4, Figures S10 and S11). Irradiation at 355 nm had a negligible and significant influence on the fluorescence behavior of the membrane under neutral and basic conditions, respectively. For this reason, membrane pieces were con-

ditioned for 24 h in buffers in the dark, and the cuvettes were kept also in the dark along the experiments.

The interaction of  $M_B$  with dopamine gives rise to the fluorescence “turn-off”, and a titration curve was obtained (Figure 1). The sensing mechanism was ascribed to a

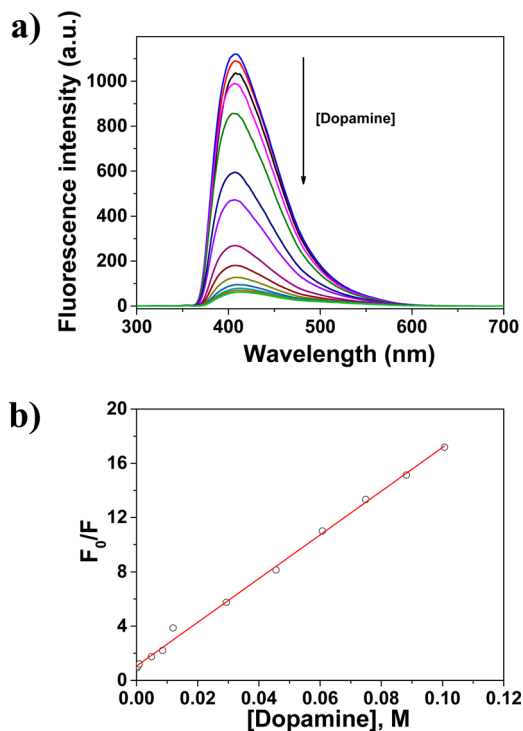


**Figure 1.** Fluorescence titration of dopamine with  $M_B$  (pH = 7, buffer = sodium phosphate monobasic): (a) fluorescence spectra of  $M_B$  upon adding increasing quantities of dopamine and (b) fluorescence quenching ( $F$  and  $F_0$  are fluorescence intensity maxima at a given concentration of dopamine and without dopamine, respectively).  $M_B$  was previously conditioned for 24 h at pH = 7 in sodium phosphate monobasic buffer in the dark. The excitation wavelength was 355 nm. The concentration of dopamine ranged from  $4.76 \times 10^{-5}$  to  $1.01 \times 10^{-1}$  M.

bimolecular deactivation or dynamic quenching that follows the Stern–Volmer equation,  $F_0/F = 1 + K_{SV}[Q]$ , where  $[Q]$  is the quencher concentration, i.e., dopamine;  $F_0$  and  $F$  are fluorescence intensity maxima in the absence and presence of dopamine, respectively; and  $K_{SV}$  is the bimolecular quenching constant. Thus,  $F_0/F$  is linearly dependent on the concentration of dopamine and the plot yields a slope and intercept of 1 on the  $y$ -axis with a slope,  $K_{SV}$ , of  $160 \text{ M}^{-1}$ . The limit of detection (LOD) was  $3 \times 10^{-4} \text{ M}$ .<sup>25</sup>

The titration of fructose and glucose gives rise to fluorescence intensity enhancement, or “turn-on”, and concomitantly to changes in the shape of emission curves and in the emission maxima wavelength.<sup>26</sup> This is caused by the formation of the cyclic boronic esters between fructose and the  $\text{Ar-B(OH)}_3^-$  motifs within the water swelled membrane (Figure 2). The ester has a stoichiometry ratio of 1:2 for fructose:monomer (**3**) in  $\text{DMSO-}d_6/\text{D}_2\text{O}$  solution, according to a Job’s plot built with  $^1\text{H}$  NMR data. The maximum of a Job’s plot representation shows the stoichiometry of a complex formed by two chemical species (e.g., a complex of two chemical species  $S$  and  $L$  with a stoichiometry of 1:2 ( $S:L$ ) would give a maximum at 0.67 when representing in the  $x$ -axis

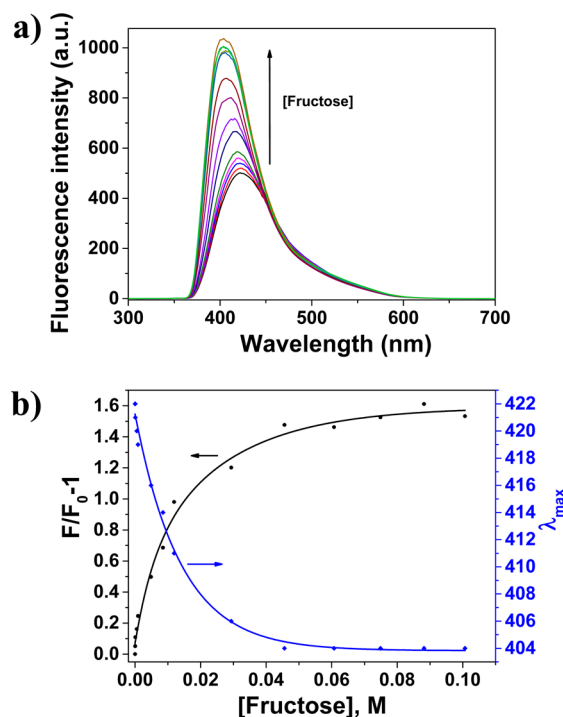


**Figure 2.** Fluorescence titration of fructose with  $M_B$  (pH = 10, buffer = sodium bicarbonate): (a) fluorescence spectra of  $M_B$  upon adding increasing quantities of fructose and (b) fluorescence intensity maxima ( $\lambda_{\text{max}}$ ) and fluorescence quenching efficiency ( $F/F_0 - 1$ , where  $F$  and  $F_0$  are fluorescence intensity at a given concentration of fructose and without fructose, respectively, at 404 nm).  $M_B$  was previously conditioned for 24 h at pH = 10 in sodium bicarbonate buffer in the dark. The excitation wavelength was 355 nm. The concentration of fructose was increased every 30 min and ranged from  $4.76 \times 10^{-5}$  to  $1.01 \times 10^{-1}$  M.

the molar fraction  $L$ ). This stoichiometry was also estimated for the interaction in the solid/gel state (membrane) of polymer pendant sensory motifs ( $\text{Ar-B(OH)}_3^-$ ) with fructose (SI, Figure S13). Similar results were obtained for glucose. The LODs were  $4 \times 10^{-4}$  and  $3 \times 10^{-4} \text{ M}$  for fructose and glucose, respectively.<sup>25</sup> Stability constants  $K_1$  and  $K_2$  for saccharide:membrane  $M_B$  complexation, i.e., solid/gel state interactions, were calculated by eq 1, where  $F$  and  $f$  are the fluorescence intensity and fluorescence proportionality factors;  $S$  and  $L$  are equilibrium concentrations inside the membrane of saccharide and pendant sensory motifs ( $\text{Ar-B(OH)}_3^-$ ); and  $SL$  and  $SL_2$  are the concentration of the 1:1 and 1:2 esters (saccharide:pendant  $\text{Ar-B(OH)}_3^-$  sensory motifs) (see SI, Section S5.3 and Figure S14) and were  $K_1 = 57$  and  $K_2 = 15$  for fructose and  $K_1 = 70$  and  $K_2 = 23$  for glucose (pH = 10, sodium bicarbonate buffer). The values of these constants points to the predominance of the complex with stoichiometry 1:1 ( $SL$ ) as depicted in the species distribution pattern (see SI, Figure S14). The estimation of stability constants of a two-phase system (solid membrane and saccharide in solution) is not straightforward, and a number of simplifications were assumed (see SI, Section S5.3). However, these simplifications were also used for the determination of the stoichiometry of the interaction in the solid state, and results were fully comparable with those obtained with monomer **3** in solution by  $^1\text{H}$  NMR (see SI, Figure S13).

$$F = \frac{-1 - K_1[S] + \sqrt{(1 + K_1[S])^2 + 8C_L K_1 K_2 [S]}}{4K_1 K_2 [S]} \left( f_L + f_{SL} K_1 [S] + f_{SL_2} \frac{-1 - K_1[S] + \sqrt{(1 + K_1[S])^2 + 8C_L K_1 K_2 [S]}}{4} \right) \quad (1)$$

The response time was about 6 min for the sensing of fructose and glucose (SI, Figure S16). The response was slower for dopamine, where 80% response (80% fluorescence quenching) was observed after 15 min (SI, Figure S15). The response time to dopamine can be lowered measuring under basic conditions, but caution is imperative because dopamine turns sensitive to oxidation in basic media.

Fluorescence spectra of the ester obtained upon interaction of saccharide with sensory motifs ( $\text{Ar-B(OH)}_3^-$ ) within the membrane at pH = 10 allowed for the discrimination between fructose and glucose, the latter establishing complexes with maximum of fluorescence red-shifted 9 nm compared with the former (Figure 3). Moreover, this discrimination can be

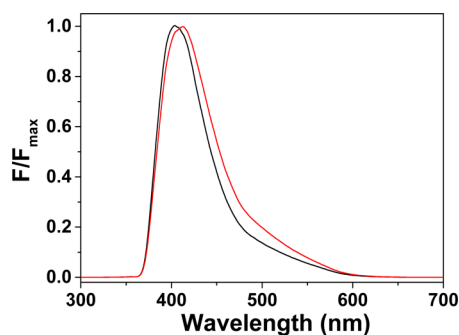


**Figure 3.** Normalized fluorescence spectra of sensory membrane  $M_B$  dipped in solutions of fructose (black) and glucose (red). The concentration of saccharides was  $1.01 \times 10^{-1}$  M (1 equiv of sensory motifs within the membrane per 2.2 equiv of saccharide).  $M_B$  was previously conditioned for 24 h at pH = 10 in sodium bicarbonate buffer in the dark. The excitation wavelength was 355 nm.

improved by comparing and analyzing all the spectra by conventional statistical data treatment, such as principal component analysis.<sup>27</sup> On the other hand, the saccharides are interference species for dopamine, even at pH = 7, diminishing its fluorescence quenching efficiency (Figure 4). However, titration curves can be obtained at a given concentration of fructose, and standard addition methods are also envisaged for determining the concentration of dopamine in the presence of saccharide interferents.

In short, we prepared a fluorescence polymer membrane as a solid sensory kit for the detection and quantification of dopamine and saccharides (glucose and fructose) in water. The sensing characteristics of the sensory membrane are based on the design of an acrylic monomer with a phenylboronic acid residue conjugated with an aromatic imino group and a phenyl ring. The detection of dopamine was carried out under neutral conditions and is based on a dynamic quenching of the fluorescence, whereas the saccharides formed under basic conditions were stable cyclic boronic esters with phenylboronic

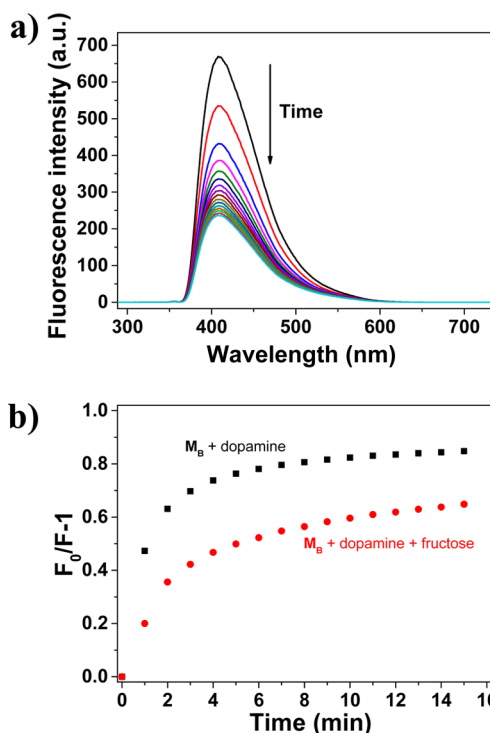


**Figure 4.** Fluorescence response time of  $M_B$  for solutions of dopamine (0.1 M) and for an equimolar solution of dopamine and fructose (0.1 M each) at pH = 7 (buffer = sodium bicarbonate): (a) fluorescence spectra along time for dopamine/fructose solution; (b) fluorescence quenching efficiency ( $F/F_0 - 1$ , where  $F$  and  $F_0$  are fluorescence intensity at 404 nm) along time of both dopamine and dopamine/fructose solutions.

acid conjugate bases ( $\text{Ar-B(OH)}_3^-$ ) with a concomitant increase in the fluorescence intensity and variations in the fluorescence maxima wavelength and fluorescence spectra patterns.

## ■ ASSOCIATED CONTENT

### Supporting Information

The Supporting Information is available free of charge on the ACS Publications website at DOI: 10.1021/acsmacrolett.5b00465.

Experimental part (measurements, intermediates, and monomer synthesis and characterization, sensory membrane preparation and characterization), study of interaction of monomer 3 with glucose, fructose and dopamine by  $^1\text{H}$  NMR, influence of light on fluorescence behavior of sensory membrane, sensing of saccharides with sensory membrane, response time studies (PDF)

## ■ AUTHOR INFORMATION

### Corresponding Author

\*Telephone number: + 34 947 25 80 85. Fax: + 34 947 25 88 31. E-mail: [jmiguel@ubu.es](mailto:jmiguel@ubu.es). <http://sites.google.com/site/grupodepolimeros/>.

### Present Address

<sup>†</sup>Polymer Photochemistry Group, Instituto de Ciencia y Tecnología de Polímeros, C.S.I.C., Juan de la Cierva 3, 28006 Madrid, Spain. E-mail: [jlpablos@ictp.csic.es](mailto:jl pablos@ictp.csic.es).

### Notes

The authors declare no competing financial interest.

## ■ ACKNOWLEDGMENTS

We gratefully acknowledge the financial support provided by the Spanish Ministerio de Economía y Competitividad-Feder (MAT2014-54137-R) and by the Consejería de Educación – Junta de Castilla y León (BU232U13).

## ■ REFERENCES

- (1) Nutt, D. J.; Lingford-Hughes, A.; Erritzoe, D.; Stokes, P. R. A. *Nat. Rev. Neurosci.* **2015**, *16*, 305–312.
- (2) Schultz, W. *Curr. Opin. Neurobiol.* **2013**, *23*, 229–238.
- (3) Nagaraja, P.; Murthy, K. C.; Rangappa, K. S.; Made Gowda, N. M. *Talanta* **1998**, *46*, 39–44.
- (4) Solich, P.; Polydorou, C. K.; Koupparis, M. A.; Efstathiou, C. E. J. *Pharm. Biomed. Anal.* **2000**, *22*, 781–789.
- (5) Varki, A.; Sharon, N. In *Essentials of Glycobiology*, 2nd ed.; Varki, A., Cummings, R. D., Esko, J. D., Freeze, H. H., Stanley, P., Bertozzi, C. R., Hart, G. W., Etzler, M. E., Eds; Cold Spring Harbor Laboratory Press: New York, 2009.
- (6) WHO, 2013. World Health Organization. ([http://www.who.int/mediacentre/fact\\_sheets/fs312/en/](http://www.who.int/mediacentre/fact_sheets/fs312/en/)).
- (7) Wang, Q.; Kamiska, I.; Niedziolka-Jonsson, J.; Opallo, M.; Li, M.; Boukherroub, R.; Szunerits, S. *Biosens. Bioelectron.* **2013**, *50*, 331–337.
- (8) Luo, J.; Luo, P.; Xie, M.; Du, K.; Zhao, B.; Pan, F.; Fan, P.; Zeng, F.; Zhang, D.; Zheng, Z.; Liang, G. *Biosens. Bioelectron.* **2013**, *49*, 512–518.
- (9) Gibson, M. I.; Neres, J.; Fullam, E. *Carbohydr. Res.* **2014**, *391*, 61–65.
- (10) Jiang, S.; Escobedo, J. O.; Kim, K. K.; Alpturk, O.; Samoei, G. K.; Fakayode, S. O.; Warner, I. M.; Rusin, O.; Strongin, R. M. *J. Am. Chem. Soc.* **2006**, *128*, 12221–12228.
- (11) Daffe, M.; Brennan, P. J.; McNeil, M. J. *J. Biol. Chem.* **1990**, *265*, 6734–6743.
- (12) Brennan, P. J.; Nikaido, H. *Annu. Rev. Biochem.* **1995**, *64*, 29–63.
- (13) Petsalakis, I. D.; Theodorakopoulos, G. *Chem. Phys. Lett.* **2013**, *586*, 111–115.
- (14) Xing, Z.; Wang, H. C.; Cheng, Y.; Zhu, C.; James, T. D.; Zhao, J. *Eur. J. Org. Chem.* **2012**, *6*, 1223–1229.
- (15) Fossey, J. S.; D’Hooge, F.; Van den Elsen, J. M. H.; Pereira Morais, M. P.; Pasco, S. I.; Bull, S. D.; Marken, F.; et al. *Chem. Rec.* **2012**, *12*, 464–478.
- (16) Guo, Z.; Shin, I.; Yoon, J. *Chem. Commun.* **2012**, *48*, 5956–5967.
- (17) Yoon, J.; Czarnik, A. W. *Bioorg. Med. Chem.* **1993**, *1*, 267–271.
- (18) Jang, Y. J.; Jun, J. H.; Swamy, K. M. K.; Nakamura, K.; Koh, H. S.; Yoon, Y. J.; Yoon, J. *Bull. Korean Chem. Soc.* **2005**, *26*, 2041–2043.
- (19) Casalini, O.; Leonardi, F.; Cramer, T.; Biscarini, F. *Org. Electron.* **2013**, *14*, 156–163.
- (20) Guo, Z.; Shin, I.; Yoon, J. *Chem. Commun.* **2012**, *48*, 5956–5967.
- (21) Egawa, Y.; Miki, R.; Seki, T. *Materials* **2014**, *7*, 1201–1220.
- (22) Roy, D.; Sumerlin, B. S. *ACS Macro Lett.* **2012**, *1*, 529–532.
- (23) Cao, K.; Jiang, X.; Yan, S.; Zhang, L.; Wu, W. *Biosens. Bioelectron.* **2014**, *52*, 188–195.
- (24) Redondo-Foj, B.; Carsi, M.; Ortiz-Serna, P.; Sanchis, M. J.; Vallejos, S.; Garcia, F.; Garcia, J. M. *Macromolecules* **2014**, *47*, 5334–5346.
- (25) The limit of detection (LOD) was estimated by the following equation:  $LOD = 3.3 \times SD/s$ , where SD is the standard deviation of a blank sample and  $s$  is the slope of the calibration curve in a region of low concentration of saccharides or dopamine.
- (26) Fang, H.; Kaur, G.; Wang, B. *J. Fluoresc.* **2004**, *14*, 481–489.
- (27) Pablos, J. L.; Sarabia, L. A.; Ortiz, M. C.; Mendia, A.; Muñoz, A.; Serna, F.; García, F. C.; García, J. M. *Sens. Actuators, B* **2015**, *212*, 18–27.